Generation of Synthetic Elastin-Mimetic Small Diameter Fibers and Fiber Networks

Lei Huang,[†] R. Andrew McMillan,[‡] Robert P. Apkarian,[‡] Benham Pourdeyhimi,[§] Vincent P. Conticello,[‡] and Elliot L. Chaikof*,[†,⊥]

Departments of Surgery and Chemistry, Emory University, School of Chemical Engineering, Georgia Institute of Technology, Atlanta, Georgia, and Department of Textile Technology, North Carolina State University, Raleigh, North Carolina

Received November 2, 1999

ABSTRACT: Elastin-mimetic peptide polymers have been synthesized, and the morphological properties of fabricated small diameter fibers and nonwoven fabrics have been characterized. An 81 kDa recombinant protein based upon the repeating elastomeric peptide sequence of elastin (Val-Pro-Gly-Val-Gly)$_4$(Val-Pro-Gly-Lys-Gly) was obtained through bacterial expression of an oligomerized gene coding for tandem repeats of the monomer. The protein was processed into fibers by an electrospinning technique and morphology defined by SEM and TEM. The choice of processing parameters influenced both fiber diameter and morphology with diameters varying between 200 and 3000 nm and three morphological patterns noted: beaded fibers, thin filaments, and broad ribbonlike structures. Detailed image analysis of nonwoven textile fabrics produced from elastin-mimetic fibers revealed that the distribution of single fiber orientation was isotropic with an associated unimodal distribution of protein fiber diameter. In a dry state, the ultimate tensile strength of nonwoven fabrics generated from elastin-mimetic peptides was 35 MPa with a material modulus of 1.8 GPa.

Introduction

As part of our program in biomimetic materials and tissue engineering, we have targeted several elements of the arterial wall as structural models for the design of an artificial blood vessel based upon the assembly of component structures. In this regard, the arterial wall can be considered in general terms a fiber-reinforced composite structure with associated mechanical properties largely a consequence of protein fiber networks. Moreover, the local mechanical environment, dictated by these network structures within the vessel wall, may in turn influence the functional responses of component cells.[1]

In tissues, such as arterial blood vessels, where energy and shape recovery are critical parameters, elastin networks dominate low-strain mechanical responses.[2] Indeed, avoidance of artery wall fatigue and failure may be dependent upon the resilience of elastin, which prevents the dissipation of transmitted pulsatile energy into heat.[3] While elastin fibers are structurally complex and may contain glycoproteins and glycosaminoglycans, the physical properties of the network have been attributed primarily to the elastin protein component produced from the soluble precursor—tropoelastin.[4] As such, Hoeve and Flory[5] demonstrated in 1974 that the driving force for the spontaneous recoil of stretched elastin is entropic in origin, consistent with classical theory of rubber elasticity. However, an apparent paradox to this conceptual picture of elastin was experimental results provided by protein chemists, which confirmed that at a supramolecular level the conformation of elastin was not that of a "random coil". Rather,
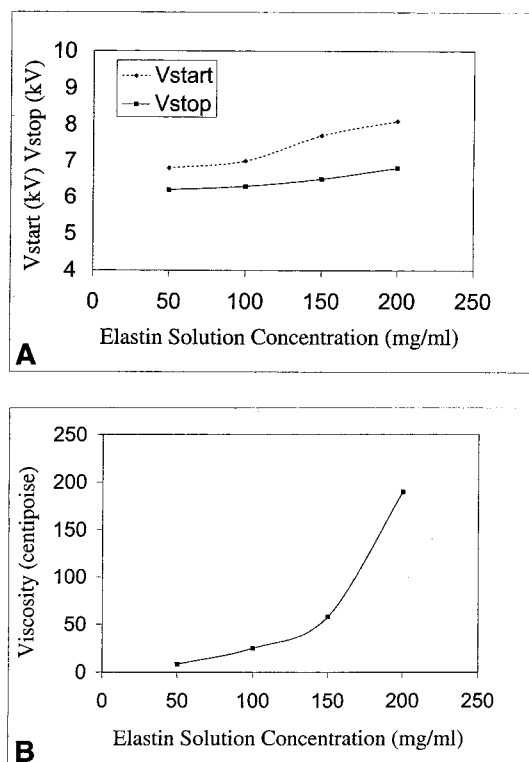

Figure 1. V_{start} and V_{stop} for various solution concentrations (A) and corresponding viscosities (B) of elastin-mimetic peptide polymer aqueous solutions.

spectroscopic studies confirmed the presence of α-helical and β-turn conformations and a twisted-rope organization imaged by electron microscopy. In resolving this paradox, extensive investigations by Urry, Tamburro, and others[4,6–18] have elaborated two different structural models for elastin consistent with its known molecular structure and the development of an entropic driving

[†] Department of Surgery, Emory University.
[‡] Department of Chemistry, Emory University.
[§] North Carolina State University.
[⊥] Georgia Institute of Technology.
* To whom correspondence should be addressed. Phone (404) 727-8413, Fax (404) 727-3660, E-mail echaiko@emory.edu.
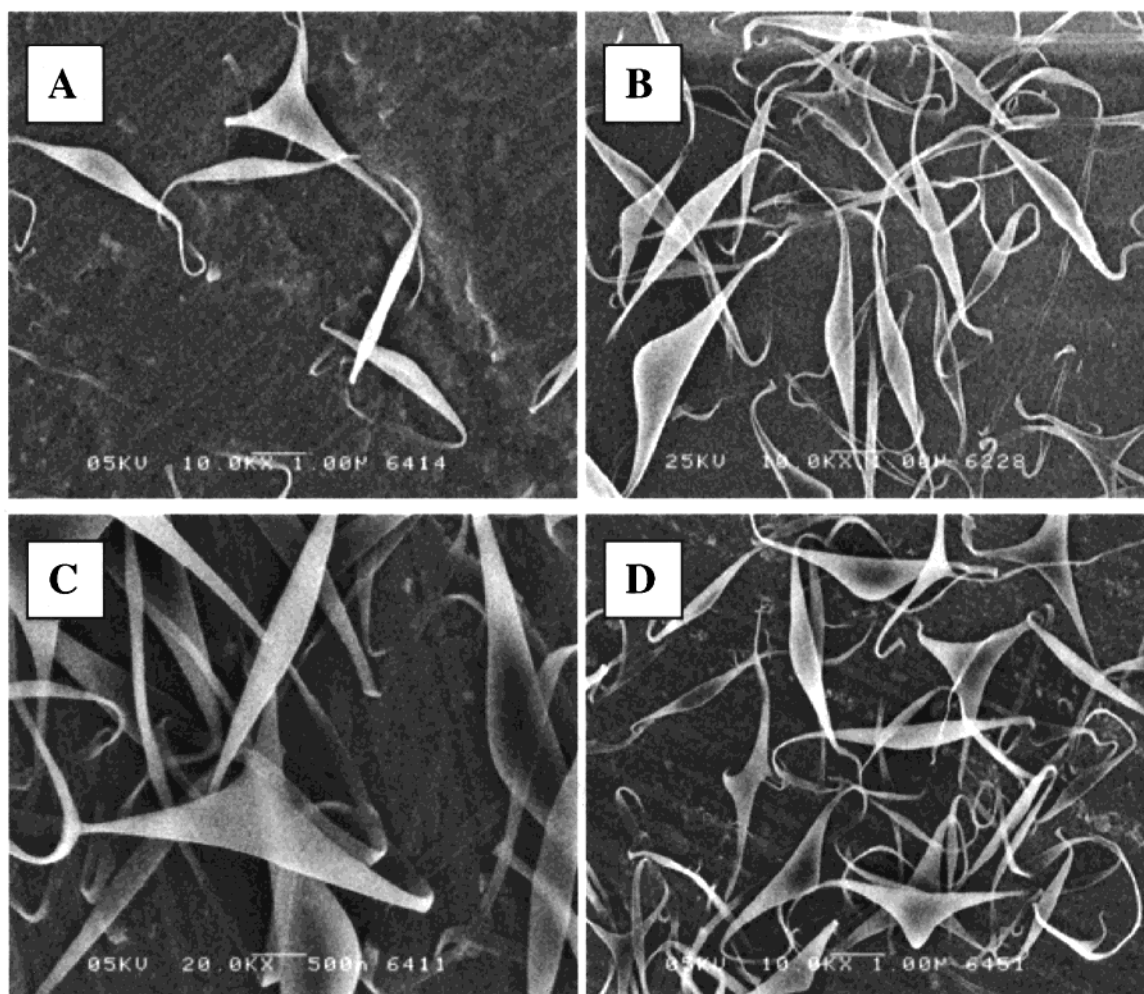
Figure 2. SEM micrographs of elastin-mimetic peptide fibers spun from 5 wt % solution at 50 (A), 100 (B), 150 (C), and 200 μL/mL (D) flow rate.

force that is responsible for its elastomeric properties. The Tamburro model is largely derived from studies of the GXGGX repeat sequence where G represents glycine and X a hydrophobic amino acid.[19,20] The model suggests that there are two major families of folded or quasi-folded structures (type I and type II β-turns, γ-turns, and half-turns) and extended or quasi-extended structures (β-sheets, polyproline II conformation) that are dynamically interchanging among themselves and, in the case of β-turns, sliding along the chain.[19,21-23] In the stretched chain, a reduction of phase-space volume and the development of hydrophobic interactions allow only high-frequency, low-amplitude motion. In structural terms this would be consistent with less flexible β-pleated sheets. On relaxation, larger amplitude motions are allowed characterized by high dynamic entropy.[24] The Urry model is based upon studies with synthetic polymers derived from the pentapeptide unit VPGVG (valine-proline-glycine-valine-glycine).[13,14] This sequence occurs frequently along the elastin chain, albeit in a different region than that containing the GXGGX sequences. The repetition of the peptide gives rise to a helical structure called a β-spiral. One type II β-turn is present per pentameric unit and, as a group, acts as spacers between dipeptide VG segments, which can undergo large-amplitude, low-frequency libations. On chain extension, a decrease in amplitude of the libations causes a large decrease in the entropy of the segment. In turn, this provides the driving force for

return to the relaxed state. The additional presence of lysine residues along the native elastin backbone also facilitates intermolecular cross-linking reactions, which likely further influences the mechanical responses of the elastin fiber network. Approximately 40% of tropoelastin lysine residues participate in cross-linking reactions.

Model polymers based upon this pentapeptide sequence have been synthesized by solution chemistry and solid-phase approaches[25] and recently by more efficient recombinant genetic engineering methodologies.[26-29] As materials, these protein polymers have been processed into elastomeric hydrogels of various forms including sheets and tubular constructs by chemical, enzymatic, and γ-irradiation mediated cross-linking of protein solutions.[14] These polymers have also been used in generating thin films. For example, both Panitch et al.[28] and Nicol et al.[30,31] have produced elastin-like protein polymers containing a periodically spaced cell binding domain. When cast from solution onto an otherwise nonadhesive substrate, these polymers promoted cell adhesion and growth. We believe that the development of efficient processing strategies, which are capable of converting elastin peptide polymers into fibers and networks that mimic native structures, will ultimately enhance the utility of these materials.

The production of fibers from protein solutions has typically relied upon the use of wet or dry spinning processes.[32,33] The latter method has been most commonly applied and involves the extrusion of a protein
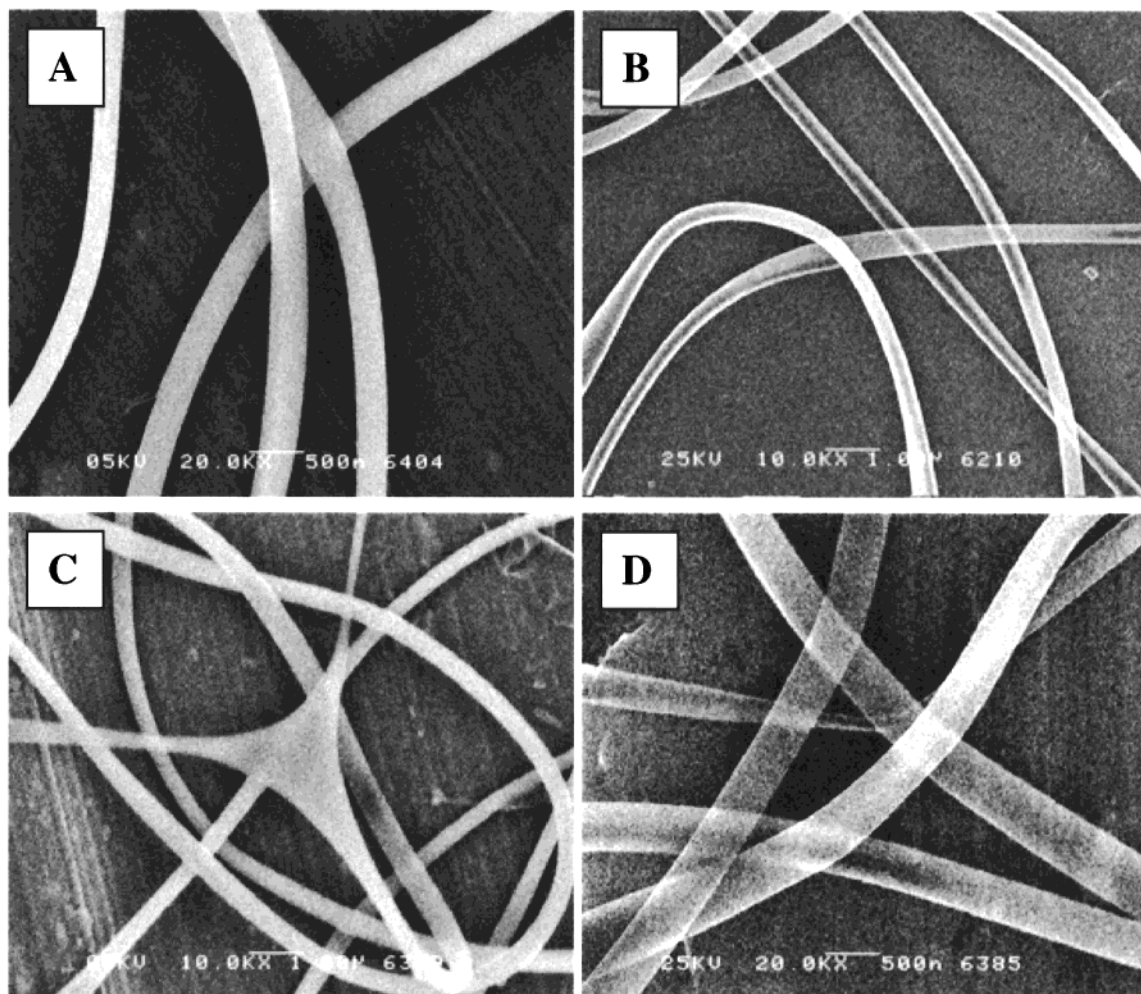
Figure 3. SEM micrographs of elastin-mimetic peptide fibers spun from 10 wt % solution at 50 (A), 100 (B), 150 (C), and 200 μL/mL (D) flow rate.

solution through a spinneret into an acid-salt coagulating bath, which usually contains aqueous ammonium sulfate, acetic acid, 2-propanol, or acetone. Alternatively, dry spinning consists of extrusion into an evaporative atmosphere. Both approaches yield large diameter fibers, which do not mimic the morphological characteristics of native protein fibers. Furthermore, both strategies rely on biologically toxic solvent systems that preclude the fabrication in real time of hybrid protein-cell constructs. Electrospinning is a third approach that has been recently utilized to generate protein fibers.[34,35] In this technique, a polymer solution is subjected to an electric field that induces the accumulation of charge on the surface of a pendent drop. Mutual charge repulsion causes a force, which directly opposes that produced by surface tension. At a critical value of electric field strength a repulsive electric force exceeds the surface tension force, and a charged jet of solution is ejected. The jet develops into a series of fine filaments with a range of diameters that are characteristically on the order of several tens or hundreds of nanometers. Given the high surface area to volume ratio of these generated nanofibers, solvent evaporation occurs as a relatively efficient process even when operating with aqueous solutions at ambient temperature and pressure. Several examples of protein nanofibers produced by the application of electrospinning techniques have been reported. Anderson et al.[36] have electrospun a series of silk-like protein polymers from formic acid and have

investigated their capacity to modify the cell adhesive characteristics of an underlying solid substrate. Likewise, Zarkoob et al.[37] have investigated the structure and morphology of regenerated B. *mori* and *N. clavipes* silk fibers produced by electrospinning.

We describe herein the first report of fiber formation from an elastin-like analogue. Electrospinning techniques were employed to produce fibers in a form that mimics native elastin fiber diameter, utilizing a 81 kDa synthetic elastin peptide polymer based upon the elastin-mimetic repeat sequence (Val-Pro-Gly-Val-Gly)$_4$(Val-Pro-Gly-Lys-Gly). The influences of process parameters on fiber morphology, including solution viscosity, flow rate, electric field strength, and the distance between the spinneret tip and the collecting surface, were defined. In addition, nonwoven fabrics based upon this elastin analogue were produced and component fiber properties including the distribution of fiber diameter and orientation characterized. A framework has been established for investigating the influence of fiber processing on both the structural features and mechanical properties of single protein fibers and fiber networks formulated as nonwoven fabrics. As a consequence, the capacity to engineer tissue like constructs whose mechanical and biological properties are based upon a hierarchical arrangement of protein networks has been significantly enhanced.
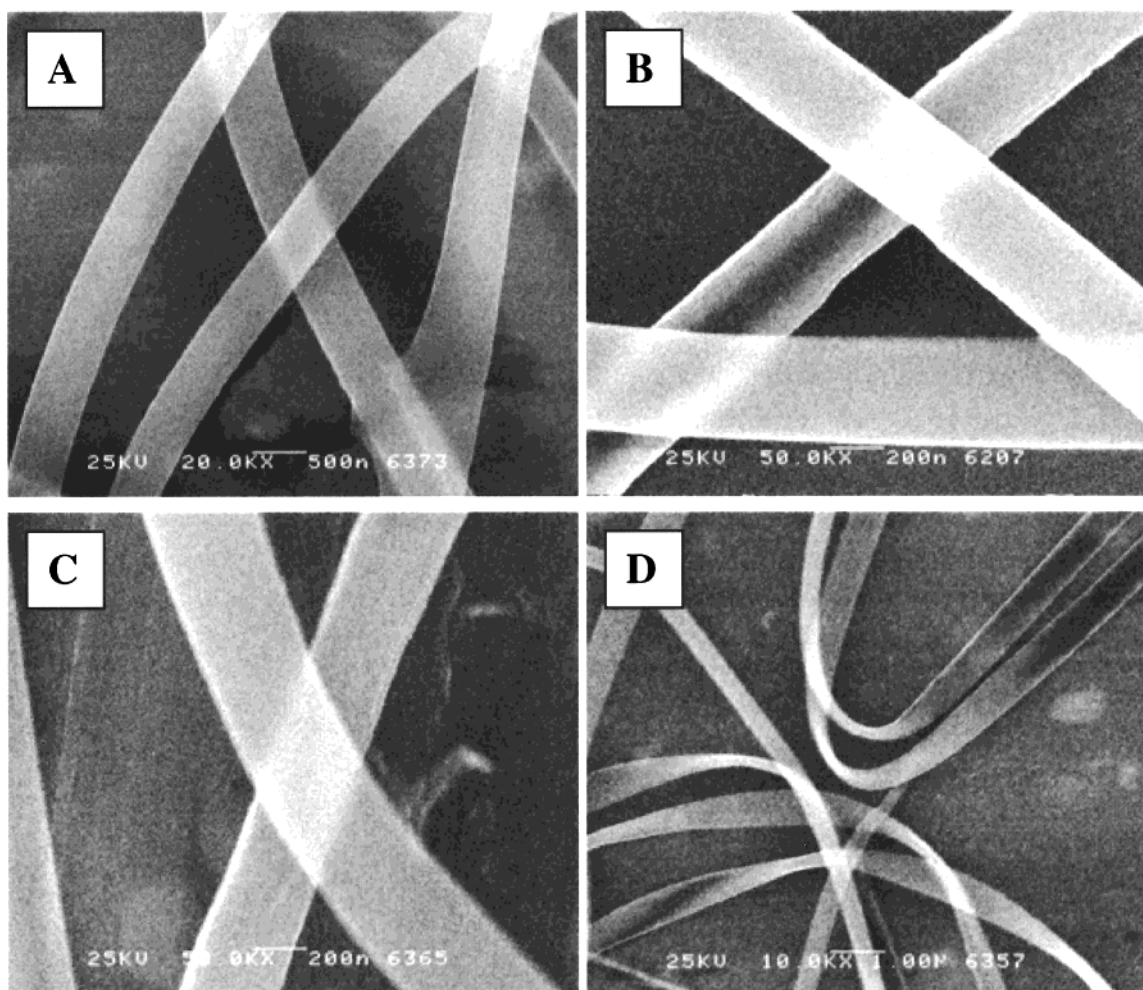
Figure 4. SEM micrographs of elastin-mimetic peptide fibers spun from 15 wt % solution at 50 (A), 100 (B), 150 (C), and 200 μL/mL (D) flow rate.

Experimental Section

Materials. An 81 kDa recombinant protein based upon the repeating elastomeric peptide sequence of elastin (Val-Pro-Gly-Val-Gly)$_4$(Val-Pro-Gly-Lys-Gly) was obtained using genetic engineering and microbial protein expression, as described in detail elsewhere.[29,38] Briefly, a concatameric gene of 3000 base pairs was isolated that encoded a repetitive polypeptide comprising 39 repeats of the elastin mimetic sequence. The protein polymer was expressed from recombinant plasmid pRAM1 in *E. coli* strain BLR(DE3) under isopropyl β-thio-galactopyranoside induction and purified to homogeneity to high yield (64 mg/L) by reversible, temperature-induced precipitation from the cell lysate. The sequence of the protein polymer has been confirmed by automated Edman degradation and MALDI-TOF mass spectroscopy of site-specific proteolytic cleavage fragments. Structural analysis of this recombinant protein has also included SDS PAGE, as well as ^{1}H and ^{13}C NMR. Low molecular weight silicone oils from Brookfield Engineering Laboratories, Inc., were used as standards for measurements of solution viscosity.

Instrumentation. An in-lens field emission scanning electron microscope (ISI DS-130F Schottky field emission SEM) was used and operated at 5 or 25 kV. High-definition topographic images at low ($\sim$1000$\times$) and medium (30 000$\times$) magnifications and high-resolution, high-magnification images ($\geq$100 000$\times$) were digitally recorded with very short dwell times and without beam-induced damage. For transmission electron microscopy (TEM) imaging a JEOL 1210 TEM was operated at 70 kV voltage. Fiber samples were deposited onto silicon chips and carbon-coated grids for scanning and transmission EM studies, respectively. Sample-containing silicon

chips were subsequently mounted onto aluminum specimen stubs with silver paste, degassed for 30 min, and coated with a 1 nm chromium (Cr) ultrathin film using a Denton DV-602 Turbo magnetron sputter system.

Preparation of Peptide Polymer Fibers. Peptide polymer solutions (5−20 wt %) were prepared in ultrafiltered grade, distilled, deionized water (18 MΩ·cm, Continental) by mixing for 12 h at 4 °C. With the aid of a syringe pump (Harvard Apparatus, Inc.), the solution was extruded at ambient temperature and pressure and at a defined flow rate through a positively charged metal blunt tipped needle (22 G $\times$ 1.5 in.). The needle was connected to a 1 mL syringe using Tygon tubing (1.6 mm i.d.). Fibers were collected on a grounded aluminum plate located below the tip of the needle. A high-voltage, low-current power supply (ES30P/DDPM, Gamma High Voltage Research, Inc.) was utilized to establish the electric potential gradient, which was varied between 0 and 30 kV, as indicated. Either positive or negative polarity can be used to run the electrospinning process. V_{start} and V_{stop}, defined as the electric potential necessary to initiate or terminate jet formation, respectively, were determined for different concentrations of elastin-mimetic peptide polymer solutions.

Image Capture of Nonwoven Fabric Samples and Analysis of Fiber Diameter and Orientation Distribution. Fabrics were generated by electrospinning at a 100 μL/min from a 15 wt % solution of elastin-mimetic peptide polymer. Specimens were placed directly on a mirror and imaged using a directional lighting arrangement where light is collimated using an "on-axis" system comprised of both a diffuser and a beam splitter. Light passes through the sample

and is reflected vertically off the mirror surface back to a CCD camera. Specular reflections from fiber surfaces do not reach the camera. Thus, fibers, regardless of their position within the fabric, merely block the light, appear dark, and are in focus. Captured images underwent segmentation or "thresholding" in order to isolate individual fibers from background. In this process, local contrast enhancement procedures were utilized including relaxation and edge thresholding techniques. Analysis also required skeletonizing of the image in which the backbone of individual fibers, corresponding to an image 1 pixel wide, was determined. Skeletonizing requires generating a "distance map" of the image that represents the minimum distance from each pixel, belonging to an object, to the background. Therefore, the highest value in the distance transform image correlates with the object center, and the peak line coincides with the axis or skeleton of the object. By using the skeleton as a guide for tracking the distance transformed image, the intensities (distances) from the fiber center to background can be determined in order to compute the diameter at all points along the skeleton. Similarly, fiber orientation is characterized by utilizing a chord-tracking algorithm, which tracks fixed small segments of individual fibers. Details of these automated image analysis techniques, as applied to fiber networks in the form of nonwoven fabrics, are provided elsewhere.[39-41] Analysis of fiber diameter and orientation distribution was based upon a minimum of 10 image fields obtained from at least two separate samples.

Stress−Strain Properties of Nonwoven Fabrics. Uniaxial tensile tests were performed on a Textechno Favimat (Herbert Stein GmbH & Co. KG, Germany). Dry samples were tested at an extension rate of 5 mm/min and an initial gage length of 10 mm. The maximum range of the load cell is 210 cN. A total of eight samples were analyzed. Samples thicknesses were determined by use of a profilometer (Tencor Alphastep 500).

Results and Discussion

Initial investigations focused on defining the electric potential necessary to initiate or terminate jet formation from aqueous solutions of the elastin analogue. Overall, values for both V_{start} and V_{stop} were proportionately related to the concentration of the peptide polymer solution and its corresponding viscosity (Figure 1). V_{start} was greater than 6.4 kV for all concentrations tested, and the splay was found to be unstable above 25 kV. Therefore, 18 kV was the chosen field strength for subsequent fiber formation investigations. Jet instability was also observed at concentrations above 20 wt % with an accompanying inability to form fibers. A systematic study of the influence on fiber morphology of the distance between the spinneret tip and the collecting plate revealed that 15 cm was an optimal distance for fiber formation.

The major determinants of fiber morphology were solution concentration and flow rate. Fibers formed from a 5 wt % solution, regardless of the mass flow rate, were short and fragmented and characterized by a triangle- or spindle-shaped beaded morphology (Figure 2). Long uniform fibers were generated at solution concentrations above 10 wt %, which corresponded to solution viscosities greater than 25 cP (Figure 3). Fiber diameters ranged between 300 and 400 nm over all flow rates tested, with little variation in morphology, with the infrequent exception of fiber splitting at triangle-shaped bifurcation points. Given a flow rate of 100 μL/min, it was estimated that 1500 m of thin filament was produced per minute. At solution concentrations of 15 and 20 wt %, a new morphological pattern was noted that was defined by the emergence of flattened or ribbon-shaped fibers, which appeared, on occasion, twisted during the spinning and deposition process
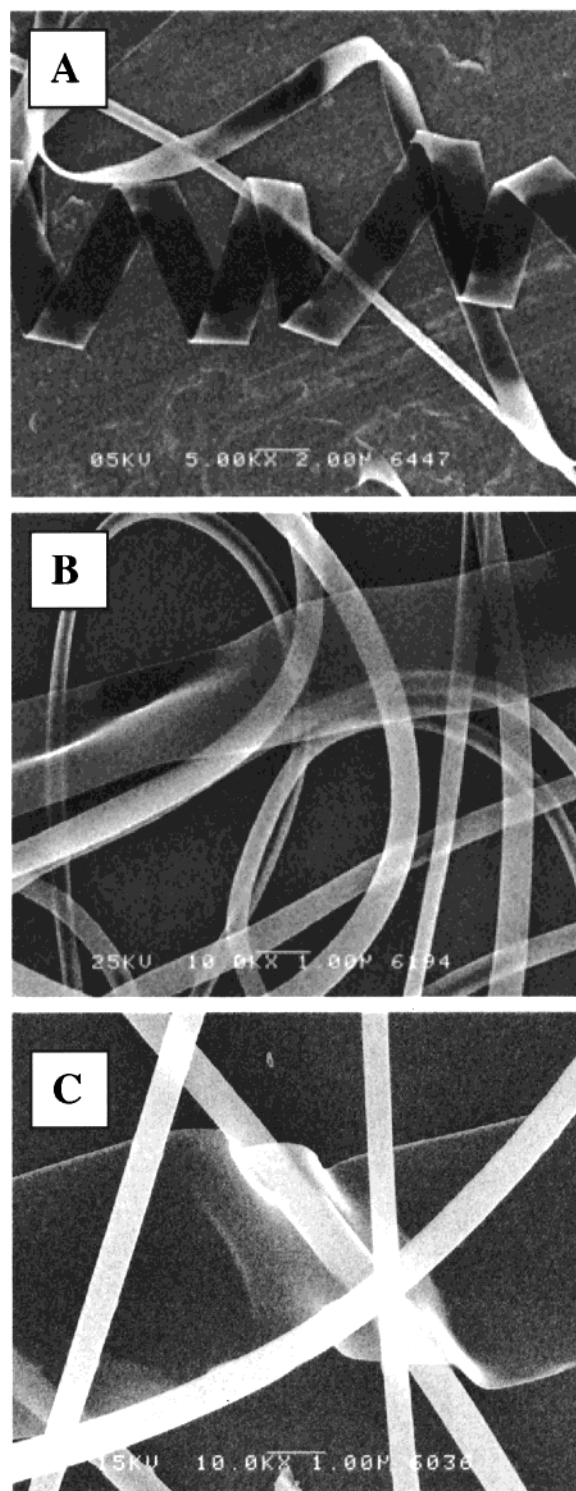

Figure 5. SEM micrographs of elastin-mimetic peptide fibers spun from 20 wt % solution at 50 (A), 100 (B), and 150 μL/mL (C) flow rate.

(Figures 4 and 5). The formation of ribbon-shaped fibers from the 20 wt % solution was a relatively common occurrence with an average fiber width of approximately 3.0 μm. However, both thin filaments (250−600 nm) and wider ribbonlike structures (~3 μm) could be observed together, particularly when fibers from this solution were formed at low flow rates. Molecular-level microstructure was observed on the surface of elastin-like ribbons, characterized by aligned axially oriented ridges with an apparent height and width of 10−20 nm (Figure
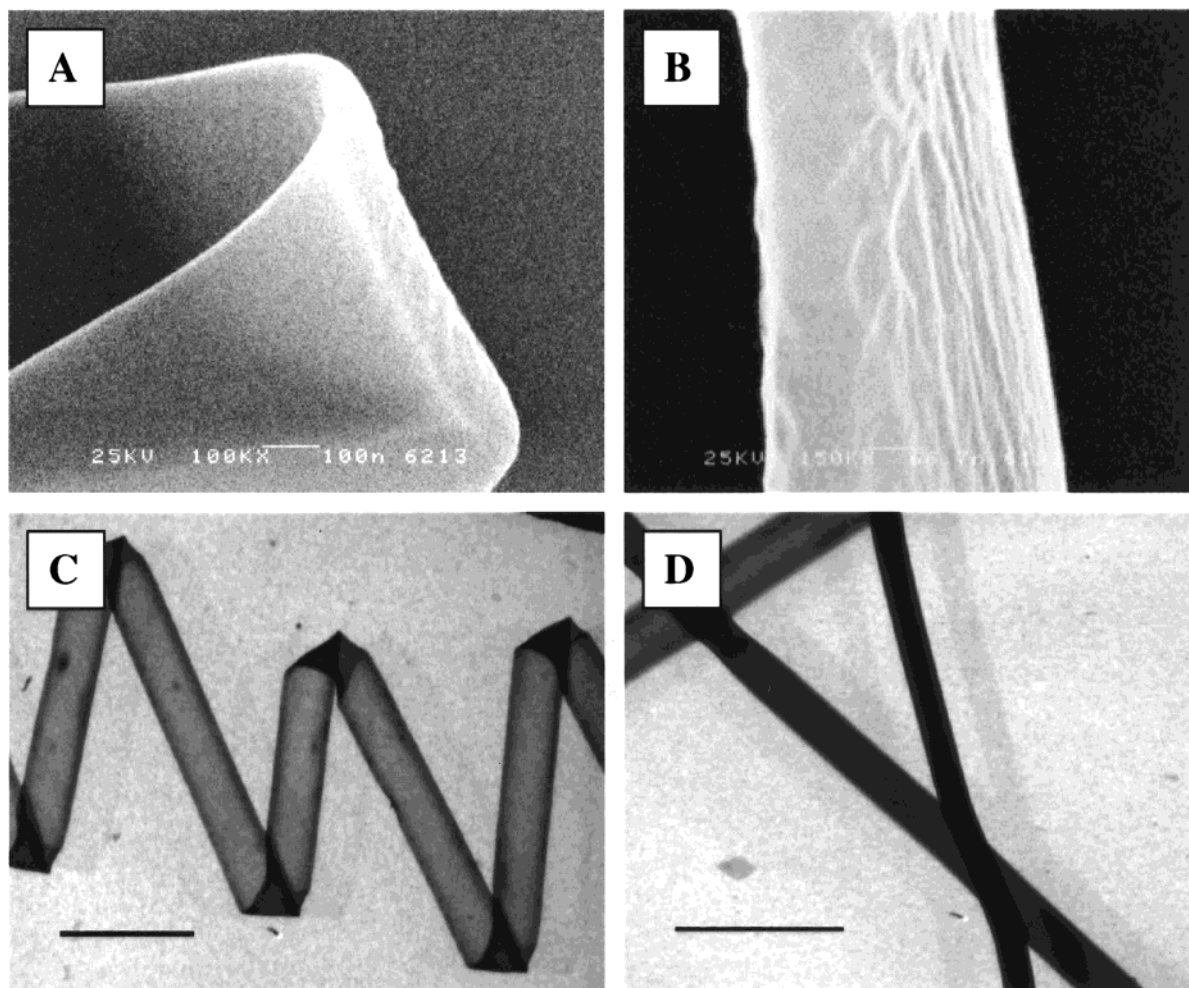
Figure 6. High-resolution SEM (A, B) and TEM (C, D) micrographs of elastin-mimetic peptide fibers spun from a 20 wt % solution at 100 μL/mL flow rate demonstrating a twisted ribbonlike morphology. Bars in parts C and D represent 3.3 and 2.0 μm, respectively.

6). Although twisted ribbons were also examined by TEM, additional higher-order structural features were not observed.

Of note, Fong et al.[42] have reported that a solution viscosity of at least 500 cP was required for effective electrospinning of nonbeaded fibers from aqueous solutions of high molecular weight poly(ethylene oxide) (MW 900 kDa). In contrast, a relatively low-viscosity solution (25 cP) of elastin peptide polymer was capable of yielding electrospun fibers of uniform diameter. This phenomenon may be related to molecular self-assembly processes that are operative for the elastin analogue and, thereby, may be an important determinant of thin filament and ribbon formation noted at low and high solution concentrations, respectively. Urry et al.[8,9] have noted that the central "Pro-Gly" element of the pentapeptide repeat (Val-Pro-Gly-Val-Gly) adopts a type II reverse turn structure, forming a flexible helix or "β-spiral" on tandem sequence repetition. Specifically, a conformational rearrangement from a random coil to a β-spiral structure has been noted for model poly-(VPGVG) peptides on phase separation of the polymer. This conformation promotes both intra- and intermolecular hydrophobic interactions and underlies the elastomeric restoring force in elastin. Therefore, during the process of nanofiber formation progressive solvent loss probably reduces the inverse transition temperature of the peptide polymer solution, consequently facilitating

both hydrophobically mediated polypeptide folding and molecular self-assembly.

Under appropriate conditions in vitro, tropoelastin molecules have a well-known tendency to aggregate into thin filaments. Likewise, the formation of elastin filaments in vivo, as basic building blocks of larger elastin fibers, has been observed by atomic force microscopy and high-resolution cryoelectron microscopy.[43,44] These studies have demonstrated that native elastin fibers can be resolved into a three-dimensional bundle of 7 nm wide filaments oriented in the direction of the fiber. It is of interest that high-resolution SEM of electrospun elastin fibers detected the presence of 10 nm wide filament-like surface folds running parallel to the direction of the fiber. Given reported electrospinning strain rates on the order of 10^4 s^{-1}, it is conceivable that elongational flow promotes the orientation and self-assembly of polymer molecules in the direction of elongation.[45] Although beyond the scope of this report, the degree to which the spinning process itself influences molecular level processes may ultimately dictate fiber structural and/or mechanical properties.

Nonwoven fabrics were formed from fibers generated from a 15 wt % of peptide polymer solution at a flow rate of 100 μL/mL (Figure 7). As noted above, short time frame deposition studies had demonstrated that these conditions afforded the highest proportion of uniform, thin fibers with diameters of approximately 400 nm.
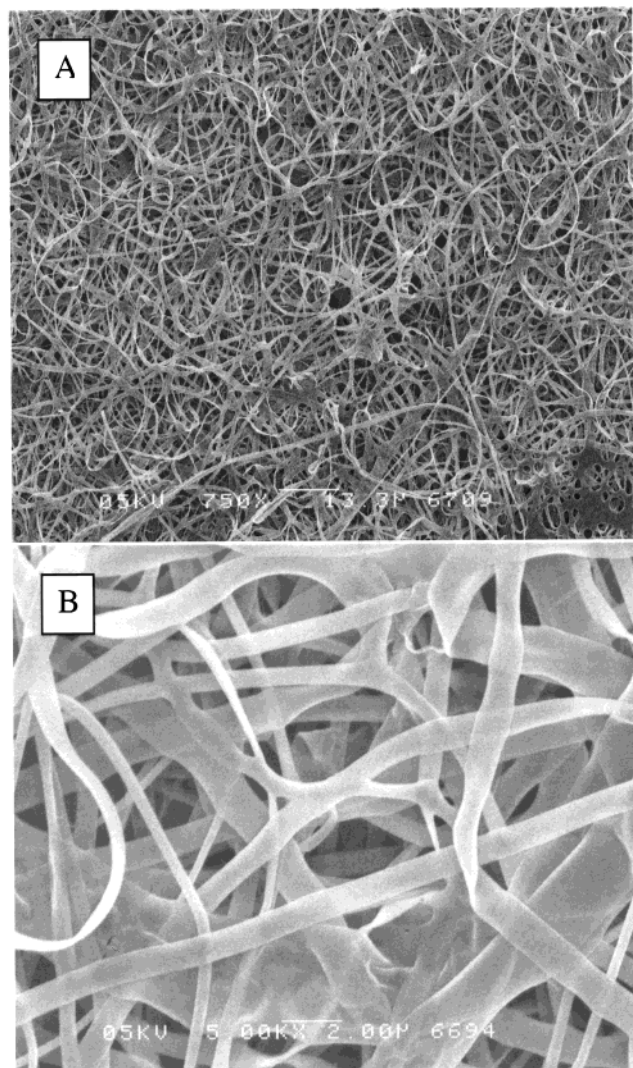
Figure 7. SEM micrographs (A, B) of a nonwoven fabric spun from a 15 wt % solution of elastin-mimetic peptide at 100 μL/mL.

Figure 8. Fiber diameter distribution within a nonwoven fabric fabric spun from a 15 wt % solution of elastin-mimetic peptide at 100 μL/mL.

Figure 9. Distribution of fiber orientation within a nonwoven fabric fabric spun from a 15 wt % solution of elastin-mimetic peptide at 100 μL/mL.

Figure 10. Representative uniaxial stress−strain curve for dry a nonwoven fabric of elastin-mimetic peptide fibers.

Image analysis of the nonwoven fabric revealed a unimodal distribution of fiber diameters with an observed average diameter of 450 nm (Figure 8). The distribution of fiber orientation within this network followed a random pattern of fiber deposition with consequent generation of an isotropic nonwoven fabric (Figure 9). Uniaxial stress−strain properties were characterized in dry nonwoven fabrics, and a representative data set is illustrated in Figure 10. The ultimate tensile strength of the sample was 35 MPa and the material modulus 1.8 GPa. Hydration and peptide cross-linking will undoubtedly modulate these properties. These studies are in progress and will be reported in due course.

Urry et al. have demonstrated that nonconservative amino acid substitutions for valine-4 can be performed without disruption of the β-spiral structure.[6,7,10,11] Thus, the incorporation of lysine in the four position of the pentapeptide and subsequent synthesis of the elastin-mimetic repeat sequence (Val-Pro-Gly-Val-Gly)$_4$(Val-Pro-Gly-Lys-Gly) permits spatially controlled chemical or enzymatic cross-linking.[38,46] The effect of polymer cross-linking on single fiber and fiber network properties is currently under investigation.
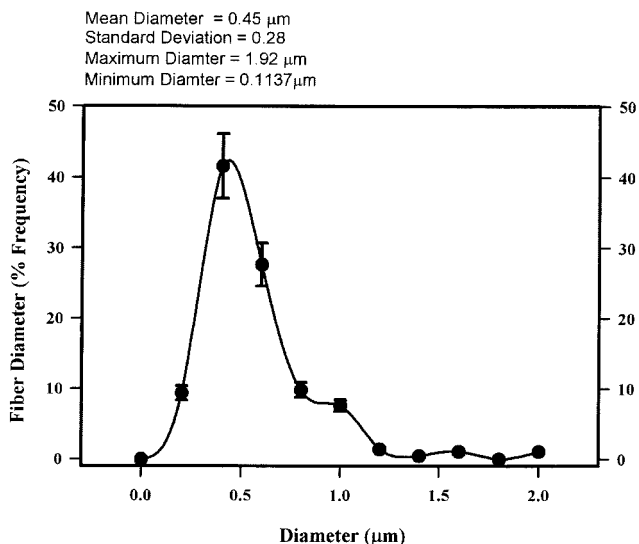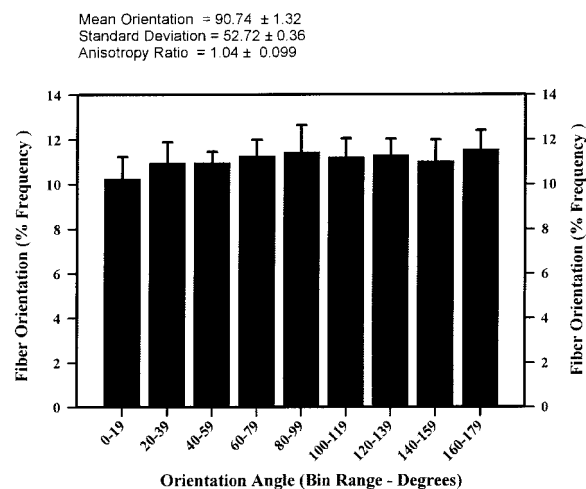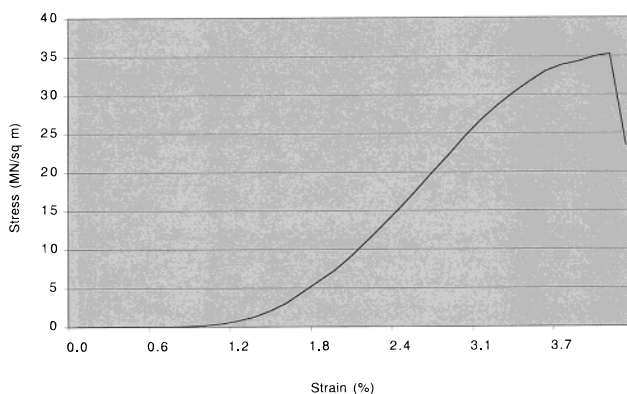
The genetic engineering of synthetic peptide polymers based upon a design derived from a native structural protein typically requires the incorporation of repetitive oligopeptide sequences that imparts critical structural properties from the parent protein to the recombinant polypeptide. In the process, model systems for investi-

gating structure−function properties of the native protein are generated. Moreover, genetic engineering based strategies facilitate the alteration of peptide chain length, consensus repeat sequence, and the introduction of additional functional groups or oligopeptide units that may modulate the biological, thermodynamic, and mechanical properties of the peptide polymer. For example, the appropriate choice of peptide sequence has led to the development of recombinant proteins that self-assemble into thermoreversible gels,[47] lyotropic smectic mesophases,[48] and lamellar crystallites.[49] Significantly, the uniformity of macromolecular structure achieved by this approach provides exquisite control over macroscopic polymer properties, including processability. The successful generation of fibers from elastin-mimetic peptide polymers has established a unique opportunity to characterize the physiochemical and biological properties of both single fibers, as well as structures with higher levels of architectural order. In particular, the creation of fiber-reinforced composites based upon a careful choice of protein polymer types and network structures may lead to the engineering of improved human tissue constructs, as well as completely synthetic artificial organs with enhanced clinical performance capabilities.

Conclusions

Elastin-mimetic protein fibers and fiber networks were produced by the electrospinning of an aqueous solution of a genetically engineered 81 kDa peptide polymer based upon the repeat sequence (Val-Pro-Gly-Val-Gly)$_4$(Val-Pro-Gly-Lys-Gly). Fibers were generated at ambient temperature and pressure with optimal fiber formation observed with use of an 18 kV electric field and a 15 cm distance between the spinneret and plate collector. High-resolution SEM and TEM confirmed that fiber morphology was primarily influenced by solution concentration and mass flow rate. Characteristically, fiber diameters varied between 200 and 3000 nm, and three morphological patterns were noted: beaded fibers, thin filaments, and broad ribbonlike structures. At solution concentrations above 10 wt % long uniform fibers were predominantly observed. Image analysis of nonwoven fabrics produced from a solution concentration of 15 wt % revealed the isotropic orientation of individual fibers with an average fiber diameter of 450 nm. The ultimate tensile strength of these nonwoven fabrics was 35 MPa and the material modulus 1.8 GPa.

References and Notes

(1) Silver, F. H.; Kato, Y. P.; M., O.; Wasserman, A. J. *J. Long-Term Effects Med. Implants* **1992**, *2*, 165−198.

(2) Roach, M. R.; Burton, A. L. *Can. J. Biochem. Physiol.* **1957**, *35*, 681−690.

(3) Sandberg, L. B.; Soskel, N. T.; Leslie, J. G. *N. Engl. J. Med.* **1981**, *304*, 566−579.

(4) Debelle, L.; Tamburro, A. M. *Int. J. Biochem. Cell Biol.* **1999**, *31*, 261−272.

(5) Hoeve, C. A.; Flory, P. J. *Biopolymers* **1974**, *13*, 677−86.

(6) Urry, D. W.; Shaw, R. G.; Prasad, K. U. *Biochem. Biophys. Res. Commun.* **1985**, *130*, 50−57.

(7) Thomas, G. J. J.; Prescott, B.; Urry, D. W. *Biopolymers* **1987**, *26*, 921−934.

(8) Urry, D. W. *J. Protein Chem.* **1988**, *7*, 1−34.

(9) Chang, D. K.; Urry, D. W. *Chem. Phys. Lett.* **1988**, *147*, 395−400.

(10) Urry, D. W.; Chang, D. K.; Krishna, N. R.; Huang, D. H.; Trapane, T. L.; Prasad, K. U. *Biopolymers* **1989**, *28*, 819−833.

(11) Chang, D. K.; Venkatachalarn, C. M.; Prasad, K. U.; Urry, D. W. *J. Biomol. Struct. Dyn.* **1989**, *6*, 851−858.

(12) Urry, D. W. *Angew. Chem., Int. Ed. Engl.* **1993**, *32*, 819−841.

(13) Urry, D. W.; Luan, C.-H.; Peng, S. Q. *Ciba Foundation Symp.* **1995**, *192*, 4−30.

(14) Urry, D. W., Luan, C.-H., Harris, C. M., Parker, T. M., McGrath, K., Kaplan, D., Eds.; Birkhauser: Boston, 1997; pp 133−177.

(15) Sandberg, L. B.; Gray, W. R.; Foster, J. A.; Torres, A. R.; Alvarez, V. L.; Janata, J. *Adv. Exp. Med. Biol.* **1977**, *79*, 277.

(16) Foster, J. A.; Bruenger, E.; Gray, W. R.; Sandberg, L. B. *J. Biol. Chem.* **1973**, *248*, 2876.

(17) Sandberg, L. B.; Leslie, J. G.; Leach, C. T.; Torres, V. L.; Smith, A. R.; Smith, D. W. *Pathol. Biol.* **1985**, *33*, 266−274.

(18) Wasserman, Z. R.; Salernme, F. R. *Biopolymers* **1990**, *29*, 1613−1628.

(19) Lelj, F.; Tamburro, A. M.; Villani, V.; Grimaldi, P.; Guantieri, V. *Biopolymers* **1992**, *32*, 161−72.

(20) Tamburro, A. M.; Guantieri, V.; Pandolfo, L.; Scopa, A. *Biopolymers* **1990**, *29*, 855−70.

(21) Villani, V.; Tamburro, A. M. *J. Biomol. Struct. Dyn.* **1995**, *12*, 1173−202.

(22) Martino, M.; Bavoso, A.; Saviano, M.; Di Blasio, B.; Tamburro, A. M. *J. Biomol. Struct. Dyn.* **1998**, *15*, 861−75.

(23) Broch, H.; Moulabbi, M.; Vasilescu, D.; Tamburro, A. M. *J. Biomol. Struct. Dyn.* **1998**, *15*, 1073−91.

(24) Villani, V.; Tamburro, A. M. *Ann. N. Y. Acad. Sci.* **1997**, *879*, 284−287.

(25) Urry, D. W.; Prasad, K. U. *Synthesis, Characterizations and Medical Uses of the Polypentapeptide of Elastin and Its Analogues*; William, D. F., Ed.; CRC Press: Boca Raton, FL, 1985.

(26) McPherson, D. T.; Morrow, C.; Minehan, D. S.; Wu, J.; Hunter, E.; Urry, D. W. *Biotechnol. Prog.* **1992**, *8*, 347−52.

(27) McPherson, D. T.; Xu, J.; Urry, D. W. *Protein Expression Purif.* **1996**, *7*, 51−7.

(28) Panitch, A.; Yamaoka, T.; Fournier, M. J.; Mason, T. L.; Tirrell, D. A. *Macromolecules* **1999**, *32*, 1701−1703.

(29) McMillan, R. A.; Lee, T. A. T.; Conticello, V. P. *Macromolecules* **1999**, *32*, 3643−3648.

(30) Nicol, A.; Gowda, D. C.; Urry, D. W. *J. Biomed. Mater. Res.* **1992**, *26*, 393−413.

(31) Nicol, A.; Gowda, D. C.; Parker, T. M.; Urry, D. W. *J. Biomed. Mater. Res.* **1993**, *27*, 801−10.

(32) Martin, D. C.; Tao, J.; Buchko, C. J. In *Processing and Characterization of Protein Polymers*; McGrath, K., Kaplan, D., Eds.; Birkhauser: Boston, 1997; pp 339−370.

(33) Hudson, S. M. In *The Spinning of Silk-like Proteins into Fibers*; McGrath, K., Kaplan, D., Eds.; Birkhauser: Boston, 1997; pp 313−337.

(34) Reneker, D. H.; Chun, I. *Nanotechnology* **1996**, *7*, 216−223.

(35) Doshi, J.; Reneker, D. H. *J. Electrostat.* **1995**, *35*, 151−160.

(36) Anderson, J. P.; Nilsson, S. C.; Rajachar, R. M.; Logan, R.; Weissman, N. A.; Martin, D. C. In *Bioactive Silk-like Protein Polymer Films on Silicon Devices*; Alper, M., Bayby, H., Kaplan, D., Navia, M., Eds.; Materials Research Society: Pittsburgh, PA, 1994; Vol. 330, pp 171−177.

(37) Zarkoob, S.; Reneker, D. H.; Eby, R. K.; Hudson, S. D.; Ertley, D.; Adams, W. W. *Polym. Prepr. (Am. Chem. Soc., Div. Polym. Chem.)* **1998**, *39*, 244−245.

(38) McMillan, R. A.; Conticello, V. P. *Macromolecules*, submitted.

(39) Pourdehyimi, B.; Dent, R.; Jerbi, A.; Tanaka, S.; Deshpande, A. *Textile Res. J.* **1999**, *69*, 185−192.

(40) Pourdeyhimi, B.; Dent, R. *Textile Res. J.* **1999**, *69*, 233−236.

(41) Pourdeyhimi, B.; Dent, R. *Textile Res. J.,* in press.

(42) Fong, H.; Chun, I.; Reneker, D. H. *Polymer* **1999**, *40*, 4585−4592.

(43) Pasquali-Ronchetti, I.; Fornieri, C.; Baccarani-Contri, M.; Quaglino, D. *Ciba Foundation Symp.* **1995**, *192*, 31−50.

(44) Pasquali-Ronchetti, I.; Allessandrini, A.; Baccarani-Contri, M.; Fornieri, C.; Mori, G.; Quaglino, D.; Valdrè, U. *Matrix Biol.* **1998**, *17*, 75−83.

(45) Reneker, D. H.; Srinivasan, G. *Bull. Am. Phys. Soc.* **1995**, *40*, 351.

(46) Kagan, H. M.; Tseng, L.; Trackman, P. C.; Okamoto, K.; Rapaka, R. S.; Urry, D. W. *J. Biol. Chem.* **1980**, *255*, 3656.

(47) Petka, W. A.; Harden, J. L.; McGrath, K. P.; Wirtz, D.; Tirrell, D. A. *Science* **1998**, *281*, 389−92.

(48) Yu, S. M.; Conticello, V. P.; Zhang, G.; Kayser, C.; Fournier, M. J.; Mason, T. L. *Nature* **1997**, *389*, 167−70.

(49) Krejchi, M. T.; Atkins, E. D. T.; Waddon, A. J.; Fournier, M. J.; Mason, T. L.; Tirrell, D. A. *Science* **1994**, *265*, 1427−1432.